2018 21st International Conference on Intelligent Transportation Systems (ITSC)
Maui, Hawaii, USA, November 4-7, 2018

# Varying Speed Limit Control of Aw-Rascle-Zhang Traffic Model

Huan Yu, Miroslav Krstic

*Abstract*— **This paper develops Varying Speed Limit(VSL) boundary control to reduce stop-and-go oscillations in congested traffic. The macroscopic traffic dynamics are governed by Aw-Rascle-Zhang(ARZ) model, consisting of second-order nonlinear partial differential equations(PDEs). The linear stability of uniform density and velocity of the ARZ model with relaxation term is discussed. Under certain densities in congested regime, small perturbations from the equilibrium transport upstream of traffic and grow into instabilities. To stabilize the inhomogeneous ARZ model around the uniform steady states, a boundary control input through VSL at outlet is considered. Using spatial transformation and backstepping method, we design a full-state feedback control law. By taking boundary measurement of density variation at the outlet, a collocated boundary observer is designed to estimate states on freeway segment. Therefore, we obtain the output feedback controller by combining the full state feedback control and collocated boundary observer. The exponential stability in $L_2$ sense and finite time convergence to equilibrium are achieved with boundary control law and boundary observer. In the end, we validate our result with simulation.**

## I. Introduction

The stop-and-go traffic is a common phenomenon in congested freeway, causing increase consumptions of fuel and unsafe driving conditions. The oscillations appear with no apparent road change, can simply be caused by delay of a driver's response. It is of great importance if we can stabilize this kind of instability in traffic flow. The traffic congestion on freeway has been investigated intensively with different levels of traffic model. Macroscopic modeling of traffic dynamics using PDEs has been proposed, including first-order model by Ligthill and Whitham and Richards, second-order Payne-Whitham model and second-order Aw-Rascle Zhang model [1] [2]. The traffic instabilities, also known as "jamiton", [3] [4] [5] [6] [7] are well represented by ARZ model, which consists of second-order, nonlinear hyperbolic PDEs of traffic density and velocity. To explore the mechanism behind this, linear stability analysis of uniform steady states of the nonlinear hyperbolic ARZ model is performed in this paper. We find that instabilities appear under certain densities in the congested regime of the ARZ model. The oscillations of density travel with vehicles while the oscillations of velocity travel upstream of the traffic.

Control strategies through ramp metering and varying speed limits are widely and effectively used nowadays in freeway traffic management [6] [8] [9] [10] [11]. In developing boundary feedback control through ramp metering and varying speed limits, many recent efforts are focused on ARZ model, due to its simplicity and realism. In [6], spectral analysis is applied to the linearized ARZ model and a parameter comparable to Froude number is proposed to classify different regimes in traffic flow. The boundary control and measurement are designed based on the spectral analysis. [8] investigates the local stability of a positive hyperbolic system with application to the ARZ model and [9] provides a boundary control law that achieves global stabilization. The control strategy developed in [6] [8] both needed coordination of ramp metering and varying speed limits. The previous cited results [8] [9] considered the homogeneous ARZ model, neglecting the relaxation term which reflects adaptation of driver's behavior to traffic conditions. Note that only the inhomogeneous ARZ model considering the delay of driver's response show the instabilities of uniform states.

In this paper, the full state feedback boundary input is implemented through VSL at the outlet to stabilize the ARZ model and collocated boundary observer is designed with measurement of outlet density. Inhomogeneous ARZ model is a nonlinear hyperbolic PDE system. We linearize it around a uniform steady density-velocity equilibrium and obtain a $2 \times 2$ coupled hyperbolic PDE system. Boundary control laws and boundary observers using backstepping method have been designed for this system [12] [13] [14] [15] and in general hetero-directional hyperbolic systems in [16] [17] [18] [19] [20]. We adopt the methodology and develop full-state feedback boundary control law and boundary observer. The contribution of this paper is two-fold. This is the first result on VSL feedback boundary control of inhomogeneous ARZ model to authors knowledge. On the other hand, this result paves the way for addressing stop-and-go traffic problem with PDE boundary control, as one of its most important application.

The outline of this paper is as follows: Section 2 introduces the inhomogeneous ARZ model and linearized it around uniform steady states. Section 3 present the linear stability analysis of the ARZ model. Under some densities in the congested regime, the uniform steady states are unstable. Sections 4 gives the full-state feedback control design with backstepping method. Section 5-6 provide boundary observer design and then the output feedback control design. Section 6 validates the previous design with simulation. Section 7 summarizes the key results of this paper.

## II. Problem statement

We consider the macroscopic Aw-Rascle-Zhang model with relaxation term on a freeway segment. The inhomogeneous ARZ model is a second-order nonlinear hyperbolic PDE system that describing the dynamics of traffic density and velocity. To study the stability of uniform density and velocity on freeway, we linearize the ARZ model around equilibrium density and velocity from the Greenshield model.

978-1-7281-0323-5/18/$31.00 ©2018 IEEE

### A. Aw-Rascle-Zhang model

The Aw-Rascle-Zhang model of $(\rho(x,t), v(x,t))$-system is given by

$$\partial_t \rho + \partial_x(\rho v) = 0, \tag{1}$$

$$\partial_t v + (v - \rho p'(\rho))\partial_x v = \frac{V(\rho) - v}{\tau}. \tag{2}$$

The state variable $\rho(x,t)$ is the traffic density and $v(x,t)$ is the traffic speed, and $\tau$ is the relaxation time. It shows how drivers' behavior adapts to equilibrium. The variable $p(\rho)$ is defined as the traffic pressure, an increasing function of density

$$p(\rho) = c_0 (\rho)^\gamma, \tag{3}$$

and $c_0, \gamma \in \mathbb{R}_+$. The equilibrium velocity-density relationship $V(\rho)$ is given in Greenshield model,

$$V(\rho) = v_f \left(1 - \frac{\rho}{\rho_m}\right), \tag{4}$$

where $v_f$ is the free flow velocity, $\rho_m$ is the maximum density and $v^\star = V(\rho^\star)$. We consider a constant traffic flux $q^\star = \rho^\star v^\star$ entering the domain from $x = 0$ and there is a VSL at the outlet. Therefore, we have the following boundary conditions,

$$\rho(0,t) = \frac{q^\star}{v(0,t)}, \tag{5}$$

$$v(L,t) = U(t) + v^\star. \tag{6}$$

where $U(t)$ is defined as variation from steady state velocity. The VSL at outlet shows $v^\star$ with $U(t)$ which we will design later. We linearize the model around uniform steady states $(\rho^\star, v^\star)$. The variations $(\tilde{\rho}(x,t), \tilde{v}(x,t))$ are defined as

$$\tilde{\rho}(x,t) = \rho(x,t) - \rho^\star, \tag{7}$$

$$\tilde{v}(x,t) = v(x,t) - v^\star. \tag{8}$$

The linearized ARZ model is given by,

$$\partial_t \tilde{\rho} + v^\star \partial_x \tilde{\rho} = -\rho^\star \partial_x \tilde{v}, \tag{9}$$

$$\partial_t \tilde{v} - (\rho^\star p'(\rho^\star) - v^\star)\partial_x \tilde{v} = \frac{\tilde{\rho} V'(\rho^\star) - \tilde{v}}{\tau}, \tag{10}$$

with the linearized boundary conditions

$$\tilde{\rho}(0,t) = -\frac{\rho^\star}{v^\star}\tilde{v}(0,t), \tag{11}$$

$$\tilde{v}(L,t) = U(t). \tag{12}$$

## III. Stability analysis of linearized ARZ model

We analyze stability of the linearized ARZ model to the uniform reference. Applying Fourier transform in $x$ and Laplace transform in t, we have

$$\tilde{\rho}(x,t) = \rho(k) \exp\left(\frac{\mathrm{i}kx}{L} + \lambda(k)t\right), \tag{13}$$

$$\tilde{v}(x,t) = v(k) \exp\left(\frac{\mathrm{i}kx}{L} + \lambda(k)t\right), \tag{14}$$

Substituting into (9) (10), we obtain

$$\begin{pmatrix} \lambda + \frac{\mathrm{i}kv^\star}{L} & \frac{\mathrm{i}k\rho^\star}{L} \\ -\frac{V'(\rho^\star)}{\tau} & \lambda + \frac{\mathrm{i}k(v^\star - \rho^\star p'(\rho^\star))}{L} + \frac{1}{\tau} \end{pmatrix} \begin{pmatrix} \rho(k) \\ v(k) \end{pmatrix} = \begin{pmatrix} 0 \\ 0 \end{pmatrix}.$$

To obtain the $k$th pair of eigenvalues, we need to solve the quadratic equation,

$$\begin{aligned} 0 =& \lambda^2 + \left(\frac{2v^\star - \rho^\star p'(\rho^\star)}{L}\mathrm{i}k + \frac{1}{\tau}\right)\lambda \\ & - \frac{v^\star(v^\star - \rho^\star p'(\rho^\star))}{L^2}k^2 + \frac{v^\star + \rho^\star V'(\rho^\star)}{\tau L}\mathrm{i}k. \end{aligned} \tag{15}$$

The discriminant is given by

$$\Delta = \left(\frac{\rho^\star p'(\rho^\star)}{L}\mathrm{i}k\right)^2 - \frac{2\rho^\star(2V'(\rho^\star) + p'(\rho^\star))}{\tau L}\mathrm{i}k + \left(\frac{1}{\tau}\right)^2. \tag{16}$$

When we consider

$$p'(\rho^\star) = -V'(\rho^\star) \implies \Delta = \left(\frac{\rho^\star p'(\rho^\star)}{L}\mathrm{i}k + \frac{1}{\tau}\right)^2, \tag{17}$$

there are two sets of eigenvalues

$$\lambda_1 = \frac{\rho^\star p'(\rho^\star) - v^\star}{L}\mathrm{i}k, \tag{18}$$

$$\lambda_2 = -\frac{1}{\tau} - \frac{v^\star}{L}\mathrm{i}k. \tag{19}$$

The real parts of two eigenvalues are non-positive and therefore the linearized ARZ model is stable. The linearized model over ($\rho^\star$, $v^\star$) is unstable when the following inequality is satisfied

$$p'(\rho^\star) < -V'(\rho^\star) \implies \Delta > \left(\frac{\rho^\star p'(\rho^\star)}{L}\mathrm{i}k + \frac{1}{\tau}\right)^2. \tag{20}$$

Then there is a positive real part appearing in $\lambda_1$.

$$\mathrm{Re}(\lambda_1) = \frac{1}{2}\left(-\frac{1}{\tau} + \mathrm{Re}(\sqrt{\Delta})\right) > \frac{1}{2}\left(-\frac{1}{\tau} + \frac{1}{\tau}\right) = 0. \tag{21}$$

From the above stability analysis, we can conclude that the linearized ARZ model is unstable under the condition that

$$p'(\rho^\star) < -V'(\rho^\star). \tag{22}$$

Thus the following inequality for uniform steady density and parameters of traffic model stands as a condition for linear instability

$$\frac{\gamma p^\star}{\rho^\star} < \frac{v_f}{\rho_m}. \tag{23}$$

Furthermore, we consider the congested regime for this problem in which $\tilde{\rho}$ transport downstream and $\tilde{v}$ transport upstream,

$$\rho^\star p'(\rho^\star) = \gamma p^\star > v^\star. \tag{24}$$

In congested regime, the linearized ARZ model around some uniform reference $(\rho^\star, v^\star)$ in the congested regime is unstable. The conditions on uniform density in (23), (24)

yield that

$$\rho^\star < \sqrt[\gamma-1]{\frac{v_f}{\gamma c_0 \rho_m}}, \tag{25}$$

$$\gamma c_0 \rho^{\star\gamma} + \frac{v_f}{\rho_m}\rho^\star - v_f > 0. \tag{26}$$

If we have $\gamma = 1$, the choice of $c_0$ should be

$$\frac{v^\star}{\rho^\star} < c_0 < \frac{v_f}{\rho_m}. \tag{27}$$

From above linear stability analysis, we also conclude that the homogeneous ARZ model does not possess instabilities and inhomogeneous ARZ model shows stop-and-go instabilities under certain densities and parameters which relate to properties of drivers. The control objective is to stabilize this unstable congested linearized ARZ model to uniform density and velocity through boundary control.

## IV. VSL FULL-STATE FEEDBACK CONTROL

Before we apply boundary control to the linearized ARZ model in (9)-(12), we represent the system in the Riemann coordinates and then map it to a decoupled first-order $2 \times 2$ hyperbolic system. We then propose the full state feedback control law for the decoupled system.

### A. Linearized ARZ model in Riemann coordinates

We first write the linearized Aw-Rascle-Zhang model in the following Riemann coordinate $(\tilde{w}, \tilde{v})$,

$$\tilde{w} = \frac{\gamma p^\star}{\rho^\star}\tilde{\rho} + \tilde{v}, \tag{28}$$

$$\tilde{v} = \tilde{v}, \tag{29}$$

thus we have

$$\partial_t \tilde{w} + v^\star \partial_x \tilde{w} = -c_1 \tilde{w} + c_2 \tilde{v}, \tag{30}$$

$$\partial_t \tilde{v} - (\gamma p^\star - v^\star)\partial_x \tilde{v} = -c_1 \tilde{w} + c_2 \tilde{v}, \tag{31}$$

$$\tilde{w}(0,t) = -r_0 \tilde{v}(0,t), \tag{32}$$

$$\tilde{v}(L,t) = U(t), \tag{33}$$

where the constants $c_1, c_2, r_0$ are defined as

$$c_1 = \frac{1}{\tau}\frac{v_f}{\rho_m}\frac{\rho^\star}{\gamma p^\star}, \tag{34}$$

$$c_2 = \frac{1}{\tau}\left(\frac{v_f}{\rho_m}\frac{\rho^\star}{\gamma p^\star} - 1\right), \tag{35}$$

$$r_0 = \frac{\gamma p^\star - v^\star}{v^\star}. \tag{36}$$

Due to instability condition in (23), the constants satisfy following inequalities

$$c_1 > \frac{1}{\tau} > 0, \tag{37}$$

$$c_2 = c_1 - \frac{1}{\tau} > 0. \tag{38}$$

According to (24), it holds that

$$r_0 > 0. \tag{39}$$

Then we scale the states to cancel the diagonal term on the right hand side so that we can apply backstepping transformation later,

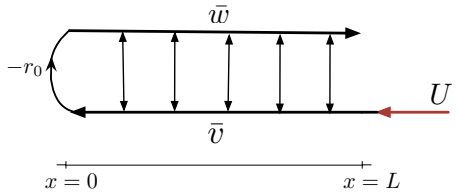


Fig. 1. Time response of VSL control model

$$\bar{w} = \exp\left(\frac{c_1}{v^\star}x\right)\tilde{w}, \tag{40}$$

$$\bar{v} = \exp\left(\frac{c_2}{\gamma p^\star - v^\star}x\right)\tilde{v}. \tag{41}$$

We have a first-order $2 \times 2$ hyperbolic system in $(\bar{w}, \bar{v})$ with in-domain spatially varying coupling,

$$\partial_t \bar{w} + v^\star \partial_x \bar{w} = \bar{c}_1(x)\bar{v}, \tag{42}$$

$$\partial_t \bar{v} - (\gamma p^\star - v^\star)\partial_x \bar{v} = \bar{c}_2(x)\bar{w}, \tag{43}$$

$$\bar{w}(0,t) = -r_0 \bar{v}(0,t), \tag{44}$$

$$\bar{v}(L,t) = r_1 U(t). \tag{45}$$

The spatially-varying coefficients are defined as

$$\bar{c}_1(x) = \exp\left(\frac{c_1}{v^\star}x - \frac{c_2}{\gamma p^\star - v^\star}x\right)c_2, \tag{46}$$

$$\bar{c}_2(x) = -\exp\left(\frac{c_2}{\gamma p^\star - v^\star}x - \frac{c_1}{v^\star}x\right)c_1, \tag{47}$$

and the constant coefficient at outlet is

$$r_1 = \exp\left(\frac{c_2}{\gamma p^\star - v^\star}L\right). \tag{48}$$

The schematic diagram of the coupled second PDE is shown in fig.1. Summarizing the transformations between $(\tilde{\rho}, \tilde{v})$-system and $(\bar{w}, \bar{v})$-system in (42)-(45), we have

$$\bar{w}(x,t) = \exp\left(\frac{c_1}{v^\star}x\right)\left(\frac{\gamma p^\star}{\rho^\star}\tilde{\rho}(x,t) + \tilde{v}(x,t)\right), \tag{49}$$

$$\bar{v}(x,t) = \exp\left(\frac{c_2}{\gamma p^\star - v^\star}x\right)\tilde{v}(x,t), \tag{50}$$

and thus the inverse transformation is given by

$$\tilde{\rho}(x,t) = \frac{\rho^\star}{\gamma p^\star}\exp\left(-\frac{c_1}{v^\star}x\right)\bar{w}(x,t) - \frac{\rho^\star}{\gamma p^\star}\exp\left(-\frac{c_2}{\gamma p^\star - v^\star}x\right)\bar{v}(x,t), \tag{51}$$

$$\tilde{v}(x,t) = \exp\left(-\frac{c_2}{\gamma p^\star - v^\star}x\right). \tag{52}$$

### B. Backstepping method for boundary control design

In order to decouple the $(\bar{w}, \bar{v})$-system in (42)-(45), we apply backstepping transformation,

$$\alpha(x,t) = \bar{w}(x,t) - \int_0^x K_{11}(x,\xi)\bar{w}(\xi,t)d\xi - \int_0^x K_{12}(x,\xi)\bar{v}(\xi,t)d\xi, \tag{53}$$

$$\beta(x,t) =\bar{v}(x,t) - \int_0^x K_{21}(x,\xi)\bar{w}(\xi,t)d\xi - \int_0^x K_{22}(x,\xi)\bar{v}(\xi,t)d\xi, \tag{54}$$

where the kernels $K_{ij}(x,\xi), i,j=1,2$ evolve in the triangular domain $\mathcal{T}=\{(x,\xi):0\le\xi\le x\le L\}$ and are governed by the following equations

$$\partial_x K_{11} + \partial_\xi K_{11} = -\frac{\bar{c}_2(\xi)}{v^\star}K_{12}, \tag{55}$$

$$v^\star\partial_x K_{12} - (\gamma p^\star - v^\star)\partial_\xi K_{12} = -\bar{c}_1(\xi)K_{11}, \tag{56}$$

$$(\gamma p^\star - v^\star)\partial_x K_{21} - v^\star\partial_\xi K_{21} = \bar{c}_2(\xi)K_{22}, \tag{57}$$

$$\partial_x K_{22} + \partial_\xi K_{22} = \frac{\bar{c}_1(\xi)}{\gamma p^\star - v^\star}K_{21}, \tag{58}$$

$$K_{11}(x,0) = -K_{12}(x,0), \tag{59}$$

$$K_{12}(x,x) = \frac{\bar{c}_1(x)}{\gamma p^\star}, \tag{60}$$

$$K_{21}(x,x) = -\frac{\bar{c}_2(x)}{\gamma p^\star}, \tag{61}$$

$$K_{22}(x,0) = -K_{21}(x,0), \tag{62}$$

The well-posedness of the kernel equations and the boundedness of the kernel variables can be proved by following the same steps of proof in [12], using method of characteristics and successive approximations. Therefore, it follows the invertibility of the backstepping transformation in (53),(54). We can study the stability of target system due to its equivalence to the plant. The target system is given by

$$\partial_t\alpha + v^\star\partial_x\alpha = 0, \tag{63}$$

$$\partial_t\beta - (\gamma p^\star - v^\star)\partial_x\beta = 0, \tag{64}$$

$$\alpha(0,t) = -r_0\beta(0,t), \tag{65}$$

$$\beta(L,t) = 0, \tag{66}$$

It is straightforward to prove the target system is exponential stable in $L_2$ and the finite-time convergence to the equilibrium can be proved by solving the target system directly in the following. The explicit solution to the target system (63)-(66) is given by

$$\alpha(x,t) = \begin{cases} \alpha(x - v^\star t, 0), & t < \frac{x}{v^\star}, \\ \alpha\left(0, t - \frac{x}{v^\star}\right), & t \ge \frac{x}{v^\star}, \end{cases} \tag{67}$$

and for $t \ge \frac{x}{v^\star}$,

$$\alpha(x,t) \equiv \alpha\left(0, t - \frac{x}{v^\star}\right) = -r_0\beta\left(0, t - \frac{x}{v^\star}\right). \tag{68}$$

Solving for $\beta(x,t)$, we have

$$\beta(x,t) = \begin{cases} \beta(x + (\gamma p^\star - v^\star)t, 0), & t < \frac{L-x}{\gamma p^\star - v^\star}, \\ \beta\left(L, t - \frac{L-x}{\gamma p^\star - v^\star}\right), & t \ge \frac{L-x}{\gamma p^\star - v^\star}, \end{cases} \tag{69}$$

Thus for $t \ge \frac{L-x}{\gamma p^\star - v^\star}$, it holds that

$$\beta(x,t) \equiv 0. \tag{70}$$

According to (68) and (70), it holds that for $t \ge t_f$,

$$\alpha(x,t) \equiv 0, \tag{71}$$

$$\beta(x,t) \equiv 0, \tag{72}$$

where the finite time constant $t_f$ is defined as

$$t_f = \frac{L}{v^\star} + \frac{L}{\gamma p^\star - v^\star}. \tag{73}$$

The convergence to equilibrium is reached in the finite time $t_f$ given in (73). The control law is obtained by evaluating (54) at $x = L$ given in (66),

$$U(t) = \frac{1}{r_1}\int_0^L K_{21}(L,\xi)\bar{w}(\xi,t)d\xi + \frac{1}{r_1}\int_0^L K_{22}(L,\xi)\bar{v}(\xi,t)d\xi. \tag{74}$$

Substituting the transformation (49),(50) between $(\bar{w},\bar{v})$-system and $(\tilde{\rho},\tilde{v})$-system into (74), we have the full-state feedback control law in the original variables $(\tilde{\rho},\tilde{v})$,

$$U(t) = \int_0^L m_1(\xi)\tilde{\rho}(\xi,t)d\xi + \int_0^L m_2(\xi)\tilde{v}(\xi,t)d\xi, \tag{75}$$

where $m_1(\xi)$ and $m_2(\xi)$ are defined as

$$m_1(\xi) = \frac{1}{r_1}K_{21}(L,\xi)\exp\left(\frac{c_1}{v^\star}\xi\right)\frac{\gamma p^\star}{\rho^\star}, \tag{76}$$

$$m_2(\xi) = \frac{1}{r_1}K_{22}(L,\xi)\exp\left(\frac{c_2}{\gamma p^\star - v^\star}\xi\right) + \frac{1}{r_1}K_{21}(L,\xi)\exp\left(\frac{c_1}{v^\star}\xi\right). \tag{77}$$

Therefore, we reach the following theorem.

**Theorem 1.** *Consider system* (42)-(45) *with inital conditions* $\bar{w}_0,\bar{v}_0 \in L_2[0,L]$ *and with control law* (75) *, where the kernels* $K_{ij}(x,\xi)$ *are obtained by solving* (55)-(62)*. The equilibrium* $\bar{w}\equiv\bar{v}\equiv 0$ *is exponentially stable in the* $L_2$ *sense. The convergence to equilibrium is reached in finite time* $t = t_f$*.*

## V. Collocated boundary observer design

In the full-state feedback controller in (75), we need the knowledge of $\tilde{\rho}(x,t),\tilde{v}(x,t)$ for $x\in[0,L]$. In practice, it is unrealistic to measure density and velocity of traffic flow for every single point on freeway. Therefore, we design a collocated boundary observer for state estimation of $(\bar{w},\bar{v})$-system.

The measurement is taken for traffic density variations at $x = L$ and we define

$$\bar{Y}(t) = \tilde{\rho}(L,t). \tag{78}$$

Therefore, the value of $Y(t) = \bar{w}(L,t)$ can be obtained from

$$\begin{aligned} Y(t) =& \bar{w}(L,t), \\ =& \exp\left(\frac{c_1}{v^\star}L\right)\left(\frac{\gamma p^\star}{\rho^\star}\tilde{\rho}(L,t) + \tilde{v}(L,t)\right) \\ =& \exp\left(\frac{c_1}{v^\star}L\right)\left(\frac{\gamma p^\star}{\rho^\star}\bar{Y}(t) + U(t)\right). \end{aligned} \tag{79}$$

Then we design an observer to estimate $\bar{w}(x,t)$ and $\bar{v}(x,t)$ by constructing the following system,

$$\hat{w}_t(x,t) = -v^\star\hat{w}_x(x,t) + \bar{c}_1(x)\hat{v}(x,t)$$

$$+\lambda_c(x)(\bar{w}(L,t)-\hat{w}(L,t)), \tag{80}$$

$$\hat{v}_t(x,t) =(\gamma p^\star - v^\star)\hat{v}_x(x,t)+\bar{c}_2(x)\hat{w}(x,t) +\mu_c(x)(\bar{w}(L,t)-\hat{w}(L,t)), \tag{81}$$

$$\hat{w}(0,t) =-r_0\hat{v}(0,t), \tag{82}$$

$$\hat{v}(L,t) =r_1U(t), \tag{83}$$

where $\hat{w}$ and $\hat{v}$ are the estimates of the state variables $\bar{w}$ and $\bar{v}$. The term $\lambda_c(x)$ and $\mu_c(x)$ are output injection gains. The error system is obtained by subtracting the above estimates from (42)-(45),

$$\check{w}_t(x,t) =-v^\star\check{w}_x(x,t)+\bar{c}_1(x)\check{v}(x,t)-\lambda_c(x)\check{w}(L,t), \tag{84}$$

$$\check{v}_t(x,t) =(\gamma p^\star - v^\star)\check{v}_x(x,t)+\bar{c}_2(x)\check{w}(x,t)-\mu_c(x)\check{w}(L,t), \tag{85}$$

$$\check{w}(0,t) =-r_0\check{v}(0,t), \tag{86}$$

$$\check{v}(L,t) =0, \tag{87}$$

where $\check{w}=\bar{w}-\hat{w}$ and $\check{v}=\bar{v}-\hat{v}$. The output injection gains $\lambda_c(x)$ and $\mu_c(x)$ are designed to guarantee that the error system decays to zero. Using backstepping method, we transform the error system (84)-(87) into the following target system

$$\partial_t\check{\alpha}+v^\star\partial_x\check{\alpha} =0, \tag{88}$$

$$\partial_t\check{\beta}-(\gamma p^\star - v^\star)\partial_x\check{\beta} =0, \tag{89}$$

$$\check{\alpha}(0,t) =-r_0\check{\beta}(0,t), \tag{90}$$

$$\check{\beta}(L,t) =0. \tag{91}$$

As proved in (63)-(66), the target system is exponential stable in $L_2$ and finite-time convergent in $t_f$. The backstepping transformation is given by

$$\check{w}(x,t) =\check{\alpha}(x,t)-\int_x^L M_{11}(x,\xi)\check{\alpha}(\xi,t)d\xi -\int_x^L M_{12}(x,\xi)\check{\beta}(\xi,t)d\xi, \tag{92}$$

$$\check{v}(x,t) =\check{\beta}(x,t)-\int_x^L M_{21}(x,\xi)\check{\alpha}(\xi,t)d\xi -\int_x^L M_{22}(x,\xi)\check{\beta}(\xi,t)d\xi, \tag{93}$$

where the kernels $M_{ij}(x,\xi), i,j=1,2$ evolve in the triangular domain $\mathcal{T}=\{(x,\xi):0\le x\le\xi\le L\}$. The kernel equations are obtained by taking spatial and temporal derivatives on both sides of the transformation, plugging into the target system,

$$\partial_x M_{11}+\partial_\xi M_{11} =-\frac{\bar{c}_1(x)}{v^\star}M_{21}, \tag{94}$$

$$v^\star\partial_x M_{12}-(\gamma p^\star - v^\star)\partial_\xi M_{12} =-\bar{c}_1(x)M_{22}, \tag{95}$$

$$(\gamma p^\star - v^\star)\partial_x M_{22}-v^\star\partial_\xi M_{22} =\bar{c}_2(\xi)M_{11}, \tag{96}$$

$$\partial_x M_{22}+\partial_\xi M_{22} =\frac{\bar{c}_2(x)}{\gamma p^\star - v^\star}M_{12}, \tag{97}$$

$$M_{11}(0,\xi) =-r_0M_{21}(0,\xi), \tag{98}$$

$$M_{12}(x,x) =\frac{\bar{c}_1(x)}{\gamma p^\star}, \tag{99}$$

$$M_{21}(x,x) =-\frac{\bar{c}_2(x)}{\gamma p^\star}, \tag{100}$$

$$M_{22}(0,\xi) =-\frac{1}{r_0}M_{12}(0,\xi), \tag{101}$$

The kernel equations are well-posed and the kernel variables are bounded proved in [12]. The stability of target system is equivalent to the error system in (84)-(87). Therefore, the error system is exponential stable in $L_2$ sense and finite-time convergence to zero in $t_f$. The output injection gain $s(x)$ and $r(x)$ are given by

$$\lambda_c(x) =-v^\star M_{11}(x,L), \tag{102}$$

$$\mu_c(x) =-v^\star M_{21}(x,L). \tag{103}$$

We summarize the above results in the following theorem.

**Theorem 2.** *Consider system* (84)-(87) *with initial conditions* $\check{w}_0,\check{v}_0\in L_2[0,L]$. *The equilibrium* $\check{w}\equiv\check{v}\equiv 0$ *is exponentially stable in the* $L_2$ *sense, which implies that* $||\bar{w}(\cdot,t)-\hat{w}(\cdot,t)||\to 0$ *and* $||\bar{v}(\cdot,t)-\hat{v}(\cdot,t)||\to 0$. *The convergence to equilibrium is reached in finite time* $t=t_f$.

After obtaining the state estimates $(\hat{w},\hat{v})$, the state estimates $(\check{\rho}(x,t),\check{v}(x,t))$ of $(\tilde{\rho}(x,t),\tilde{v}(x,t))$ are obtained according to (51)(52),

$$\check{\rho} =\frac{\rho^\star}{\gamma p^\star}\exp\left(-\frac{c_1}{v^\star}x\right)\hat{w}-\frac{\rho^\star}{\gamma p^\star}\exp\left(-\frac{c_2}{\gamma p^\star - v^\star}x\right)\hat{v}, \tag{104}$$

$$\check{v} =\exp\left(-\frac{c_2}{\gamma p^\star - v^\star}x\right)\hat{v}, \tag{105}$$

and then the state estimates $(\hat{\rho}(x,t),\hat{v}(x,t))$ of $(\rho(x,t),v(x,t))$ are obtained

$$\hat{\rho}(x,t) =\check{\rho}(x,t)+\rho^\star, \tag{106}$$

$$\hat{v}(x,t) =\check{v}(x,t)+v^\star. \tag{107}$$

By taking the boundary measurement of density variations $\bar{Y}(t)=\tilde{\rho}(0,t)$, we estimate $(\bar{w},\bar{v})$ and then obtain state estimates $(\hat{\rho}(x,t),\hat{v}(x,t))$ according to above relations (104)-(107).

## VI. VMS OUTPUT FEEDBACK CONTROL

Combining the full-state feedback controller in (74) and the collocated boundary observer, we have the output feedback control law

$$U(t) =\frac{1}{r_1}\int_0^L K_{21}(L,\xi)\hat{w}(\xi,t)d\xi +\frac{1}{r_1}\int_0^L K_{22}(L,\xi)\hat{v}(\xi,t)d\xi. \tag{108}$$

where $\hat{w}$ and $\hat{v}$ can be obtained from the collocated boundary observer with measurement $\bar{Y}(t)=\tilde{\rho}(L,t)$, given in (80)-(83). The output injection gains are given in (102)(103). The kernels $K_{21}(x,\xi)$, $K_{22}(x)$ are computed by solving the kernel equation (55)-(62). The following theorem summarize the results of Theorem 1 and Theorem 2.

**Theorem 3.** *Consider system* (63)-(66) *with inital conditions* $\bar{w}_0,\bar{v}_0\in L_2[0,L]$ *and with control law, where the kernels* $K_{21}(x,\xi)$ *and* $K_{22}(x,\xi)$ *are obtained by solving*

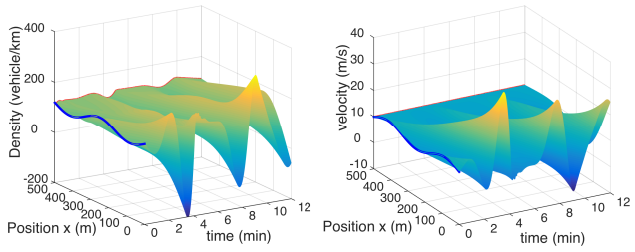


Fig. 2. Evolution of open-loop system

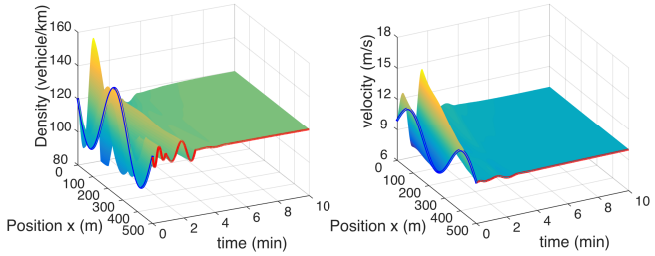


Fig. 3. Evolution of closed-loop system with VSL

(57)(58)(61)(62). *The equilibrium* $\bar{w} \equiv \bar{v} \equiv \hat{w} \equiv \hat{v} \equiv 0$ *is exponentially stable in the* $L_2$ *sense and convergence is reached in* $2t_f$. *According to transformation in* (49)-(50)*, uniform steady states* $(\rho^\star, v^\star)$ *that satisfy* (23)(24) *are exponentially stable in the* $L_2$ *sense and the convergence of* $(\rho, v)$*-system to steady states* $(\rho^\star, v^\star)$ *is reached in* $2t_f$.

## VII. Simulation

We take $\gamma = 1$ and choose $c_0$ according to (27). The length of freeway section is chosen to be $L = 500$ m. The free speed is $v_f = 40$ m/s and the maximum density is $\rho_m = 160$ vehicles/km. The steady states $(\rho^\star, v^\star)$ are chosen as $(120$ vehicles/km$, 10$ m/s$)$ which are in the congested regime. The relaxation time $\tau = 120$ s. We use sinusoid initial conditions. We run the open-loop system for 10 min.

The fig.2 below shows that in the open-loop system where there are no speed variations at the outlet where VSL works like a speed limit sign. It takes less than 1 min for vehicles to leave the freeway segment if they drive around the steady velocity $v^\star = 10$ m/s. The density and velocity disturbances grow and oscillate for 10 min even after the disturbance generating vehicles leave the domain. In practice, the traffic becomes bumper-to-bumper jammed and completely stops when density reaches its maximum and velocity reduces to zero.

Then we apply the full-state feedback VSL controller, the fig.3. shows the simulation result of closed-loop system with full-state feedback VSL control law. The closed-loop system is exponentially stable and the convergence to uniform steady states is achieved in finite time $t_f = 4$ min.

## VIII. Conclusion

This paper solves output feedback control problem of ARZ traffic model with relaxation term. The linear instability conditions of stop-and-go traffic are discussed for ARZ model. To stabilize the coupled hyperbolic PDE system, the full-state feedback control is designed with VSL controlling traffic velocity at the outlet. The collocated boundary measurement is taken for density at outlet to estimate states. We achieve exponential stability in $L_2$ sense and the finite time convergence to steady states. The key idea is to explore the control problem of stop-and-go traffic in the framework of ARZ PDE model. Boundary control with VSL is realized by applying backstepping PDE control method. An interesting extension of this work is to consider traffic congestion control problem in the presence of moving bottleneck or lane-drop.

## References


[1] Zhang, H. M. (2002). A non-equilibrium traffic model devoid of gas-like behavior. Transportation Research Part B: Methodological, 36(3), 275-290.

[2] Aw, A., & Rascle, M. (2000). Resurrection of" second order" models of traffic flow. SIAM journal on applied mathematics, 60(3), 916-938.

[3] Flynn, M. R., Kasimov, A. R., Nave, J. C., Rosales, R. R., Seibold, B. (2009). Self-sustained nonlinear waves in traffic flow. Physical Review E, 79(5), 056113.

[4] Seibold, B., Flynn, M. R., Kasimov, A. R., Rosales, R. R. (2012). Constructing set-valued fundamental diagrams from jamiton solutions in second order traffic models. arXiv preprint arXiv:1204.5510.

[5] Fan, S., Herty, M., & Seibold, B. (2013). Comparative model accuracy of a data-fitted generalized Aw-Rascle-Zhang model. arXiv preprint arXiv:1310.8219.

[6] Belletti, F., Huo, M., Litrico, X., & Bayen, A. M. (2015). Prediction of traffic convective instability with spectral analysis of the AwRascleZhang model. Physics Letters A, 379(38), 2319-2330.

[7] Kerner, B. S. (1998). Experimental features of self-organization in traffic flow. Physical review letters, 81(17), 3797.

[8] Zhang, L., & Prieur, C. (2017). Necessary and Sufficient Conditions on the Exponential Stability of Positive Hyperbolic Systems. IEEE Transactions on Automatic Control.

[9] Karafyllis, I., Bekiaris-Liberis, N., & Papageorgiou, M. (2017). Analysis and Control of a Non-Standard Hyperbolic PDE Traffic Flow Model. arXiv preprint arXiv:1707.02209.

[10] Bastin, G., & Coron, J. M. (2016). Stability and boundary stabilization of 1-d hyperbolic systems (Vol. 88). Birkhuser.

[11] Zhang, Y., & Ioannou, P. A. (2017). Coordinated variable speed limit, ramp metering and lane change control of highway traffic. IFAC-PapersOnLine, 50(1), 5307-5312.

[12] Vazquez, R., Krstic, M., & Coron, J. M. (2011, December). Backstepping boundary stabilization and state estimation of a 2 2 linear hyperbolic system. In Decision and Control and European Control Conference (CDC-ECC), 2011 50th IEEE Conference on (pp. 4937-4942). IEEE.

[13] Coron, J.-M., Vazquez, R., Krstic, M., & Bastin, G. (2013). Local exponential H2 stabilization of a 2 2 quasilinear hyperbolic system using backstepping. SIAM Journal on Control and Optimization, 51, 20052035.

[14] Deutscher, J. (2017). Output regulation for general linear heterodirectional hyperbolic systems with spatially-varying coefficients. Automatica, 85, 34-42.

[15] Yu, H., Vazquez, R., & Krstic, M. (2017). Adaptive output feedback for hyperbolic PDE pairs with non-local coupling. In American Control Conference (ACC), 2017 (pp. 487-492). IEEE.

[16] Hu, L., Di Meglio, F., Vazquez, R., & Krstic, M. (2016). Control of homodirectional and general heterodirectional linear coupled hyperbolic PDEs. IEEE Transactions on Automatic Control, 61(11), 3301-3314.

[17] Di Meglio, F., Vazquez, R., & Krstic, M. (2013). Stabilization of a system of $n + 1$ coupled first-order hyperbolic linear PDEs with a single boundary input. IEEE Transactions on Automatic Control, 58(12), 3097-3111.

[18] Meglio, F., Argomedo, F. B., Hu, L., & Krstic, M. (2016). Stabilization of coupled linear heterodirectional hyperbolic PDEODE systems.

[19] Auriol, J., & Di Meglio, F. (2016). Minimum time control of heterodirectional linear coupled hyperbolic PDEs. Automatica, 71, 300-307.

[20] Hasan, A., Aamo,O. M.,& Krstic, M.(2016). Boundary observer design for hyperbolic PDEODE cascade systems. Automatica, 68,75-86.